Molecules and Cells

Establishment and Characterization of Carboplatin-Resistant Retinoblastoma Cell Lines

Chang Sik Cho[1], Dong Hyun Jo[2], Jin Hyoung Kim[3], and Jeong Hun Kim[1,4,5,6,*]

[1]Fight against Angiogenesis-Related Blindness (FARB) Laboratory, Clinical Research Institute, Seoul National University Hospital, Seoul 03080, Korea, [2]Department of Anatomy and Cell Biology, Seoul National University College of Medicine, Seoul 03080, Korea, [3]BIOGENO KOREA, Ltd., Seoul 04376, Korea, [4]Department of Ophthalmology, Seoul National University Hospital, Seoul 03080, Korea, [5]Department of Biomedical Sciences, Seoul National University College of Medicine, Seoul 03080, Korea, [6]Institute of Reproductive Medicine and Population, Seoul National University College of Medicine, Seoul 03080, Korea
*Correspondence: steph25@snu.ac.kr
https://doi.org/10.14348/molcells.2022.2014
www.molcells.org

Carboplatin-based chemotherapy is the primary treatment option for the management of retinoblastoma, an intraocular malignant tumor observed in children. The aim of the present study was to establish carboplatin-resistant retinoblastoma cell lines to facilitate future research into the treatment of chemoresistant retinoblastoma. In total, two retinoblastoma cell lines, Y79 and SNUOT-Rb1, were treated with increasing concentrations of carboplatin to develop the carboplatin-resistant retinoblastoma cell lines (termed Y79/CBP and SNUOT-Rb1/CBP, respectively). To verify resistance to carboplatin, the degree of DNA fragmentation and the expression level of cleaved caspase-3 were evaluated in the cells, following carboplatin treatment. In addition, the newly developed carboplatin-resistant retinoblastoma cells formed *in vivo* intraocular tumors more effectively than their parental cells, even after the intravitreal injection of carboplatin. Interestingly, the proportion of cells in the G_0/G_1 phase was higher in Y79/CBP and SNUOT-Rb1/CBP cells than in their respective parental cells. In line with these data, the expression levels of cyclin D1 and cyclin D3 were decreased, whereas p18 and p27 expression was increased in the carboplatin-resistant cells. In addition, the expression levels of genes associated with multidrug resistance were increased. Thus, these carboplatin-resistant cell lines may serve as a useful tool in the study of chemoresistance in retinoblastoma and for the development potential therapeutics.

Keywords: carboplatin, cell cycle, chemoresistance, multidrug resistance, retinoblastoma

INTRODUCTION

The primary treatment option for retinoblastoma, the most common intraocular malignant tumor in children, is intravenous or intra-arterial chemotherapy and focal treatment (Abramson et al., 2015). Although a primary chemotherapy regimen based on carboplatin, vincristine and etoposide is usually sufficient (Kaliki and Shields, 2015), enucleation (the total removal of the eyeball) is still performed in select patients in which the tumor is or has become chemoresistant. In this context, there is a need for the development of effective second-line treatment options for chemoresistant retinoblastoma. To facilitate research into the mechanisms of chemoresistant tumors and develop counteractive measures to inhibit their progression, it is necessary to create a series of chemoresistant cell lines, similar to those that exist in the fields of breast and lung cancer. However, there have unfortunately only been limited attempts to develop chemoresistant retinoblastoma cell lines, which were not well characterized (Stephan et al., 2008; Wang et al., 2013).

In the present study, two carboplatin-resistant retinoblastoma cells were developed by treating two retinoblastoma cell

Received 5 November, 2021; revised 2 March, 2022; accepted 29 May, 2022; published online 29 August, 2022

eISSN: 0219-1032

lines, Y79 and SNUOT-Rb1, with increasing concentrations of carboplatin in a stepwise fashion. The carboplatin resistant Y79 and SNUOT-Rb1 cells were termed Y79/CBP and SNUOT-Rb1/CBP. The resulting Y79/CBP and SNUOT-Rb1/CBP lines exhibited both *in vitro* and *in vivo* resistance to carboplatin. In addition, in the carboplatin-resistant cells, there was an increase in the proportion of cells in the G_0/G_1 phase when compared with their respective parental cell lines. Furthermore, ATPase copper transporting (ATP7) α (*ATP7A*), *ATP7B*, ATP binding cassette subfamily (ABC) B member 1 (*ABCB1*), *ABCC1*, *ABCC2*, and *ABCG2* expression was increased in the Y79/CBP cells, and *ATP7B*, *ABCB1*, *ABCC1*, *ABCC2*, and *ABCG2* expression was increased in the SNUOT-Rb1/CBP cells, suggesting the presence of multidrug resistance (MDR) in the carboplatin-resistant cells.

MATERIALS AND METHODS

Cell culture

Retinoblastoma cell lines, Y79 (American Type Culture Collection; ATCC, USA) and SNUOT-Rb1 (Kim et al., 2007) cells were cultured in RPMI-1640 medium (Welgene, Korea) supplemented with 10% fetal bovine serum (Thermo Fisher Scientific, USA), penicillin (100 U/ml) and streptomycin (100 μg/ml) at 37°C in a humidified incubator with 95% air and 5% CO_2. Culture medium was replaced every 3 days and cells were observed daily under a phase contrast microscope (Carl Zeiss, Germany).

Establishment of carboplatin-resistant cell lines

Carboplatin-resistant cells were established by treating parental cells with gradually increasing concentrations of carboplatin, based on established methods (Asada et al., 1998; Behrens et al., 1987; Chen et al., 2013; Dallas et al., 2009; Jensen et al., 2015). Carboplatin (Cat. No. C2538; Sigma-Aldrich, USA) was added when the cells reached 70%-80% confluence. After 2 days of carboplatin exposure, medium was replaced with fresh carboplatin-free medium until the living cells had recovered. When the cells reached equal confluence, carboplatin was added again. Each concentration was repeated three times. Y79/CBP cells were treated with carboplatin at concentrations of 15.4, 46.2, 92.4, and 138.6 μM, and SNUOT-Rb1/CBP cells were treated with concentrations of 10.5, 31.5, 63, and 94.5 μM. Cells grown in each final concentration were stored for further investigation. Finally, resistant cells were maintained in 5 μM carboplatin.

Cell viability assay

Cell viability was evaluated using an EZ-Cytox (WST-1 based) assay kit according to the manufacturer's protocol (DoGenBio, Korea). Cells (1×10^4 cells/well) were seeded into 96-well plates and cultured overnight. The following day, cells were treated with carboplatin at different concentrations (50, 100, 200, 400, or 800 μM), and incubated for 48 h. WST-1 solution was added to each well and incubated at 37°C for a further 3 h. Absorbance was measured at 450 nm using a microplate reader (Thermo Fisher Scientific). Each test was performed in triplicate.

DNA fragmentation analysis

Cells (1×10^7 cells/well) were resuspended in 20 μl TES lysis buffer (20 mM EDTA, 100 mM Tris, pH 8.0, 10% SDS, 5 M NaCl). An RNAse cocktail (10 μl; 500 units/ml RNAse A and 20,000 units/ml RNAse T1) was added and incubated at 37°C for 1 h. Subsequently, 10 μl proteinase K (20 mg/ml) was added and incubated at 50°C for 1 h. DNA samples were mixed with 6× DNA loading buffer, and separated on a 2% agarose gel at 35 V for 4 h. The gel contained SYBR Safe DNA gel stain (Thermo Fisher Scientific) along with a DNA ladder, and was visualized using a Molecular Imager Gel Doc XR+ system (Cat. No. 1708195; Bio-Rad Laboratories, USA).

Immunocytochemistry

Y79 cells were plated on and allowed to attach to poly-D-lysine coated culture slides. SNUOT-Rb1 cells were seeded onto culture slides. After the cells had attached, they were washed with phosphate-buffered saline (PBS) and fixed with 4% formaldehyde for 15 min at room temperature. Subsequently, cells were permeabilized with 0.2% Triton X-100 in PBS for 5 min and washed with PBS. Slides were incubated with Universal Blocking Reagent (BioGenex, USA) for 10 min and then incubated with a cleaved caspase-3 antibody (1:1,000, Cat. No. 9664; Cell Signaling Technology, USA) overnight at 4°C. Slides were rinsed with PBS and incubated with an Alexa 488-conjugated secondary antibody (Thermo Fisher Scientific) for 1 h. Nuclear staining was performed using DAPI. Fluorescence images were acquired using a fluorescence microscope (Leica Microsystems, Germany).

Animals

Male BALB/c nude mice (age, 6 weeks) were purchased from the Central Lab Animal (Korea). Mice were provide *ad libitum* access to food and water, and were maintained in a room with a 12-h light/dark cycle. All animal experiments were performed according to the ARVO Statement for the Use of Animals in Ophthalmic and Vision Research and in accordance with the guidelines of the Seoul National University Institutional Animal Care and Use Committee. The present study was approved by the Seoul National University on January 8, 2017 (approval No. SNU-120111-8-4) and the experiments were performed between March and June 2017.

Orthotopic transplantation of retinoblastoma cells into mice and evaluation of *in vivo* chemoresistance

For *in vivo* orthotopic experiments, harvested cells were washed with PBS and suspended in serum-free RPMI-1640 medium at a density of 1×10^7 cells/ml. Zoletil (30 mg/kg; Virbac Korea, Korea) and xylazine (10 mg/kg; Bayer Korea, Korea) were injected by intraperitoneal injection into mice prior to cell injection; the use of Zoletil was supported by a previous publication (Khokhlova et al., 2017). After adequate anesthesia, 1×10^4 cells (1 μl) was injected into the vitreous cavity of the right eye of the mice (Jo et al., 2013; Kaplan et al., 2010; Laurie et al., 2005; 2009). A total of six animals were used per a group, and a total of 48 animals were used. After 2 weeks, carboplatin was injected into the eye at a concentration three times greater than its IC_{50} in the respective parental cells (Y79 and Y79/CBP, 400 μM; SNUOT-Rb1 and

SNUOT-Rb1/CBP, 300 μM). After 4 weeks, tumor formation was evaluated using the visual grading system, as described previously (Jo et al., 2017), and mice were sacrificed. Mice were exposed to 100% CO_2 concentration in an euthanasia chamber (54 L) for 10 min following the National Institutes of Health ARAC guidelines for euthanasia of rodents (30% of the chamber displaced by CO_2 per minute). Eyes were removed, embedded in paraffin and cut into 4 μm sections. These sections were stained with H&E. The tumor area was quantified using ImageJ (National Institutes of Health, USA). Data were compared using a two-way ANOVA, and are presented as the mean ± SEM.

Estimation of cell growth rate

Y79 cells were suspended in the culture medium at a density of 1×10^4/ml and plated in 12-well microplates. SNUOT-Rb1 cells were removed from the surface of the culture dish, using trypsin-EDTA, and washed with RPMI-1640 medium. Next, cells were resuspended in the culture medium at a density of 1×10^4/ml, and plated onto 12-well microplates. Cells from three wells were digested and counted every 2 days for a total of 7 days. Doubling time was calculated for each cell line according to the following equation: Doubling time = duration × $\log_2$/log(final concentration) − log(initial concentration).

Cell cycle analysis

Cells were harvested and centrifuged at 1,200 rpm for 5 min at 4°C, the supernatant was removed and the cells were carefully washed twice with PBS. Next, cells were fixed in 70% ethanol for 1 h at 4°C. Fixed cells were washed again with PBS and treated with 10 μg/ml RNase for 1 h. Subsequently, cells were stained with propidium iodide (PI) dye and examined using a BD Accuri C6 Plus flow cytometer (BD Biosciences, USA). Data were analyzed using BD Accuri C6 software (BD Biosciences). Each test was performed in triplicate.

Western blot assay

Protein concentrations were determined using a BCA protein assay kit (Thermo Fisher Scientific). Equal amounts of protein were loaded on a 10% or 12% SDS-gel, resolved using SDS-PAGE and transferred to a nitrocellulose membrane (Amersham™ Protran™; Cytiva, Korea). Membranes containing transferred proteins were incubated with antibodies against cyclin-D1 (1:1,000, Cat. No. 2978; Cell Signaling Technology), cyclin-D3 (1:1,000, Cat. No. 2936; Cell Signaling Technology), p18 (1:1,000, Cat. No. 2896; Cell Signaling Technology), p21 (1:1,000, Cat. No. 2947; Cell Signaling Technology), and β-actin (1:5,000, Cat. No. A2066; Sigma-Aldrich) overnight at 4°C. The following day, membranes were washed with PBS-Tween and incubated for 1 h at room temperature with the appropriate peroxidase-conjugated secondary antibody (Santa Cruz Biotechnology, USA). Membranes were then washed with PBS-Tween and signals were visualized using EZ-Western Lumi Pico solution (DoGenBio). Digital imaging was performed using imageQuant LAS4000 (Cytiva).

Reverse transcription-quantitative polymerase chain reaction (RT-qPCR)

Total RNA was isolated using TRIzol® reagent (Thermo Fisher Scientific), and reverse transcribed to cDNA using a High Capacity cDNA kit, according to the manufacturer's protocol (Thermo Fisher Scientific). RT-qPCR was performed using TaqMan Fast Advanced MasterMix and TaqMan probe (Thermo Fisher Scientific). GAPDH was used as the internal control for normalization. Primer and probe sets were *ABCB1* (assay ID, Hs00392137_m1), *ABCC1* (assay ID, Hs00967238_m1), *ABCC2* (assay ID, Hs01091188_m1), *ABCG2* (assay ID, Hs01053790_m1), *ATP7A* (assay ID, Hs00163707_m1), *ATP7B* (assay ID, Hs00163739_m1), and *GAPDH* (assay ID, Hs0275899_g1) (Thermo Fisher Scientific). The PCR thermocycling conditions were: 40 cycles of 20 s at 95°C for polymerase activation, denaturation for 1 s at 95°C, and 20 s at 60°C for annealing/extension. Fluorescence signals were collected at the end of the elongation step of each PCR cycle (72°C for 10 s) to monitor the quantity of amplified DNA. ΔCq was calculated from the efflux gene − the Cq of GAPDH. Next, ΔCq was calculated by subtracting the ΔCq of parental cells from the ΔCq of resistant cells. Fold change in gene expression was calculated using the $2^{-\Delta\Delta Cq}$ method.

MDR assay

Detailed protocols for MDR analysis can be found in the manual of the EFLUXX-ID Green Multidrug Resistance Assay kit (Cat. No. ENZ-51029-K100; Enzo Life Sciences, USA). Cells were harvested, counted and diluted to an equal number of cells (5×10^5) in RPMI-1640 medium. Each group was inoculated with inhibitors (verapamil, 50 μM; MK571, 100 μM; novobiocin, 100 μM) or DMSO and resuspended, followed by incubation at 37°C for 10 min. The green dye (part of the kit) was added and cells were incubated at 37°C for 30 min. To exclude dead cells from the assay, PI was added to the cells for the last 5 min. Cells were washed once with cold PBS prior to FACS analysis.

Statistical analysis

Statistical analysis was performed using Prism 9 (GraphPad Software, USA). Comparisons between groups were made using one-way ANOVA and Tukey's post-hoc multiple comparison tests. $P < 0.05$ was considered to indicate a statistically significant difference.

RESULTS

Establishment of carboplatin-resistant retinoblastoma cell lines

Y79/CBP and SNUOT-Rb1/CBP cells exhibited similar morphological characteristics to their parent cells, Y79 and SNUOT-Rb1, respectively. Only a few Y79/CBP cells were found to be enlarged compared to Y79. SNUOT-Rb1/CBP cells exhibited a slightly elongated shape. (Fig. 1A). Using western blotting, microtubule-associated protein (MAP) 2 and cone-rod homeobox (CRX) proteins were found to be highly expressed in retinoblastoma cells as well as in the parental cells (Supplementary Fig. S1A). Western blot analysis was performed to demonstrate that SNUOT-Rb1 cells were

not endothelial cells nor retinal pigment epithelial cells (Supplementary Fig. S1B). Additionally, immunohistochemistry staining revealed that MAP2, CRX and synaptophysin, which are expressed in retinoblastoma, were expressed in Y79 and SNUOT-Rb1 cells. In SNUOT-Rb1 cells, glial fibrillary acidic protein was expressed weakly in the tumor and strongly in stromal cells (Supplementary Fig. S2). By contrast, there were notable differences in carboplatin-sensitivity between the cell lines. The IC_{50} of carboplatin in the Y79 cells was 24 ± 21.46 μM, compared with 378 ± 4.46 μM in the Y79/CBP resistant cells (Fig. 1B, Supplementary Table S1). The IC_{50} of carboplatin in the SNUOT-Rb1 cells was 65 ± 2.23 μM, which increased to 325 ± 108.3 μM in the SNUOT-Rb1/CBP resistant cells (Fig. 1B, Supplementary Table S1). Furthermore, a DNA fragmen-

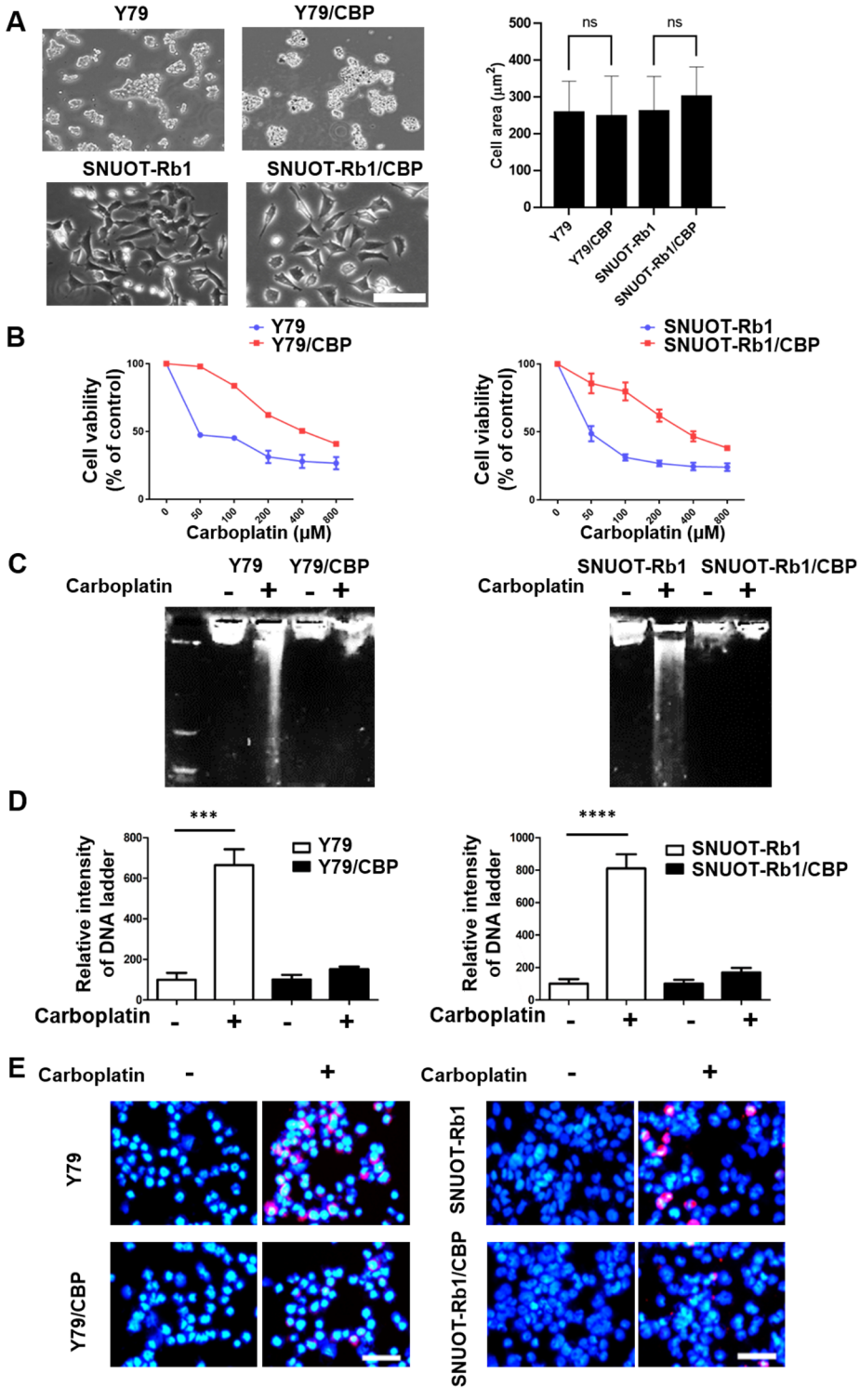

Fig. 1. Establishment of carboplatin-resistant retinoblastoma cell lines. (A) Parental and resistant cells were observed under an inverted microscope. CBP, carboplatin; ns, not significant. Scale bar = 100 μm. (B) Viability of Y79, Y79/CBP, SNUOT-Rb1, and SNUOT-Rb1/CBP cells after exposure to carboplatin for 48 h. (C) DNA fragmentation in Y79, Y79/CBP, SNUOT-Rb1, and SNUOT-Rb1/CBP cells after treatment with carboplatin for 48 h. (D) Quantification of DNA fragmentation ladder strength in arbitrary units. Statistical analysis was performed using a one-way ANOVA with a post hoc Newman-Keuls multiple comparisons test. ***$P < 0.001$; ****$P < 0.0001$. (E) Expression of cleaved caspase-3 in Y79, Y79/CBP, SNUOT-Rb1, and SNUOT-Rb1/CBP cells after treatment with carboplatin for 48 h. Scale bars = 50 μm.

tation assay demonstrated that the Y79 and SNUOT-Rb1 cells exhibited DNA fragmentation due to cell death when treated with carboplatin at concentrations three times the IC_{50} value of the parental cells, but this did not occur in the resistant cells (Figs. 1C and 1D). Under the same treatment conditions, intracellular cleaved caspase-3 was highly expressed in the parental cells, but relatively lower in the resistant cells (Fig. 1E). It was also confirmed that the apoptotic rate was lower in the resistant cells based on the Annexin V staining and flow cytometry analysis (Supplementary Fig. S3).

In vivo carboplatin-resistance of Y79/CBP and SNUOT-Rb1/CBP cells

Retinoblastoma cells (1×10^4 cells) were injected into the vitreous cavities of mice. Carboplatin was administered 2 weeks after injection of cells via the intravitreal route, and the eyeballs were evaluated for tumor formation (Fig. 2A). Carboplatin injection inhibited tumor formation in the mice injected with the parental cells, whereas tumors consisting of Y79/CBP or SNUOT-Rb1/CBP cells continued to grow after the carboplatin treatment (Fig. 2B). H&E staining confirmed differences in the *in vivo* tumor formations between the mice

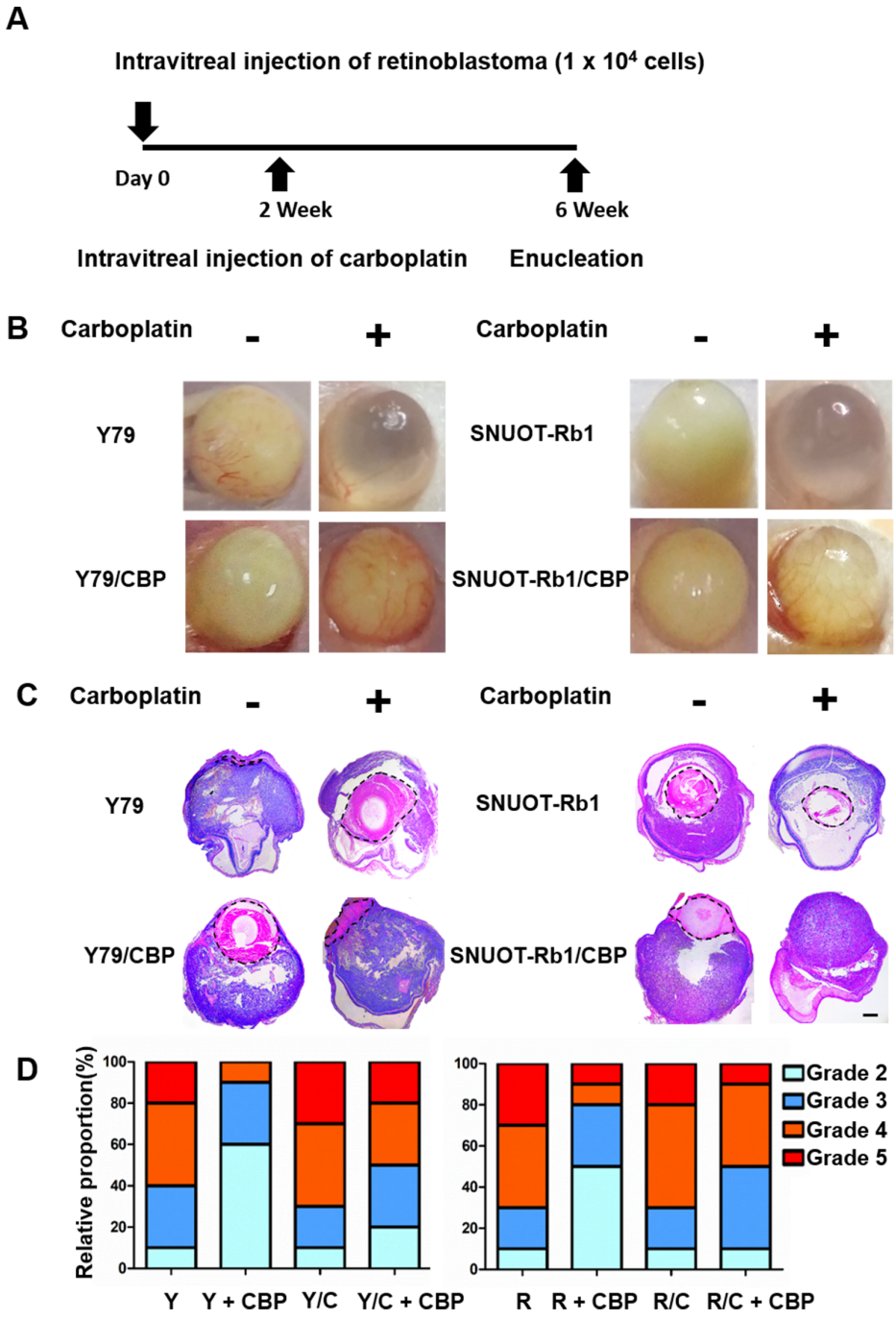

Fig. 2. *In vivo* chemoresistance of Y79/CBP and SNUOT-Rb1/CBP cells. (A) Schematic of the *in vivo* experiments. Retinoblastoma cells ($1 \times 10^4/\mu l$) were injected into the eyeballs, followed by a carboplatin injection directly into the eyeballs 2 weeks later. A total of 4 weeks after the carboplatin injection, tumor formation was evaluated and eyeballs were removed for further analysis. (B) Representative photographs of mouse eyes showing the different degrees of tumor formation. (C) Representative images of H&E staining of the *in vivo* orthotopic tumors. Scale bar = 100 μm. (D) Visual grading of the *in vivo* tumor formations in the different treatment groups. Grade 2, plaque; Grade 3, mass; Grade 4, mass filling the eyeball; Grade 5, eyeball enlargement. CBP, carboplatin; Y, Y79; Y/C, Y79/CBP; R, SNUOT-Rb1; R/C, SNUOT-Rb1/CBP.

injected with the parental and carboplatin-resistant retinoblastoma cells (Fig. 2C). In addition, the intraocular tumor size was measured and quantified for each group. The maximum tumor size obtained in the study was 9.054 mm^2 in the Y79/CBP injected mice treated with carboplatin, and 9.615 mm^2 in the SNUOT-Rb1/CBP injected mice (Supplementary Fig. S4). The visual grading system was used to assess the degree of tumor formation from 0-5 (Jo et al., 2017). According to the visual grading system, the carboplatin injected group in the parental cells was classified as Grade 2 (plaque-like tumor) and Grade 3 (definite mass formation), whereas the group injected with carboplatin-resistant cells exhibited Grade 3 and 4 tumors (vitreous-filling tumor) (Fig. 2D).

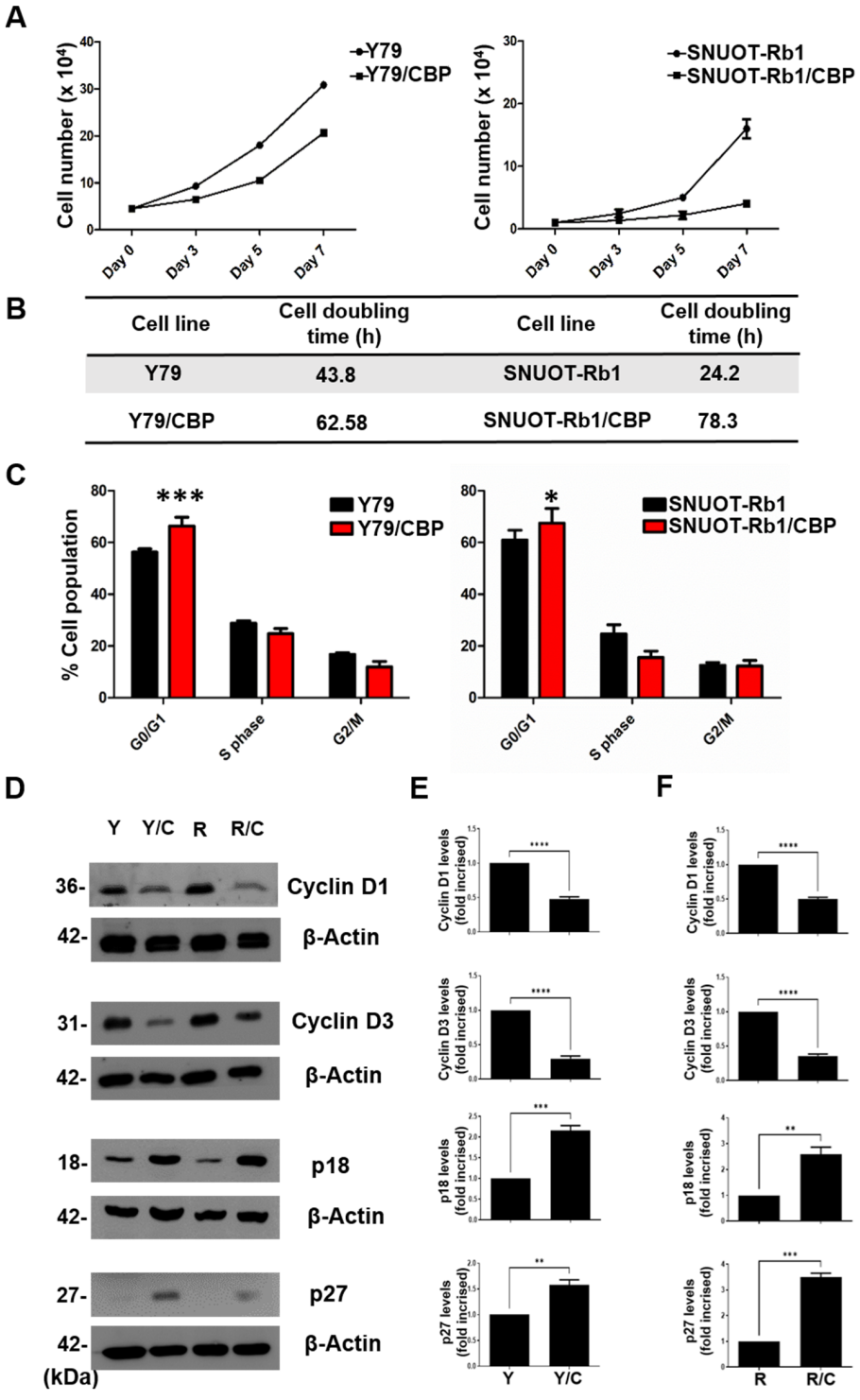

Fig. 3. Growth curves, cell cycle distribution and cell cycle protein expression in parental and resistant cells. (A) Number of cells under normal culture conditions. (B) Doubling time of a cell was estimated using the number of cells at each designated time point. (C) Proportion of cells in each cell cycle phase in Y79, Y79/CBP, SNUOT-Rb1, and SNUOT-Rb1/CBP cell populations. Statistical analysis was performed using an unpaired Student's *t*-test. (D) Expression of proteins associated with the cell cycle. (E) Semi-quantitative analysis of cell cycle-related protein expression. (F) Semi-quantitative analysis of SNUOT-Rb1 cell cycle-related protein expression. Statistical analysis was performed using an unpaired Student's *t*-test. $*P < 0.05$; $**P < 0.01$; $***P < 0.001$; $****P < 0.0001$. CBP, carboplatin; Y, Y79; Y/C, Y79/CBP; R, SNUOT-Rb1; R/C, SNUOT-Rb1/CBP.

The proportion of cells in the G_0/G_1 phase is increased in the carboplatin-resistant retinoblastoma cells

Under normal culture conditions, Y79/CBP cell counts increased 3.2× and the SNUOT-Rb1/CBP increased 1.4× more slowly than their respective parental cells (Figs. 3A and 3B). FACS showed that the proportion of cells in the G_0/G_1 phase was higher than the respective parental cells (Fig. 3C, Supplementary Fig. S5). Western blot analysis revealed that the expression levels of cyclin D1 and cyclin D3, cell cycle proteins associated with the G_0/G_1 phase, were reduced in the resistant cells when compared with the parental cells. By contrast, the expression levels of p18 and p27, inhibitors of cyclin D1 and cyclin D3, were significantly increased in the resistant cells when compared with the parental cells (Fig. 3D). Experiments were repeated three times, and semi-tquantification was performed (Figs. 3E and 3F).

Increased drug efflux in carboplatin-resistant retinoblastoma cells

To characterize the Y79/CBP and SNUOT-Rb1/CBP cells further, RT-qPCR was used to evaluate the expression of MDR-related genes in the carboplatin-resistant cells compared with the parental cells. Interestingly, the expression levels of *ABCB1*, *ABCC1*, *ABCC2*, *ABCG2*, *ATP7A*, and *ATP7B* were increased in Y79/CBP cells, and the expression levels of *ABCB1*, *ABCC1*, *ABCC2*, *ABCG2*, and *ATP7B* were increased in the SNUOT-Rb1/CBP cells compared with their parental cells (Fig. 4A). In line with these results, the Y79/CBP and SNUOT-Rb1/CBP cells exhibited increased drug efflux compared with their parental cells, which was reversed by treatment with verapamil (an MDR1 inhibitor), MK-571 (an MRP inhibitor), or novobiocin (a BCRP inhibitor) (Fig. 4B).

DISCUSSION

The cells used in the present study were the Y79 and SNUOT-Rb1 cell lines. MAP2, CRX and synaptophysin are strongly expressed in Y79 and SNUOT-Rb1 cells. These markers are also highly expressed in retinoblastomas (Bond et al., 2013; Glubrecht et al., 2009; Katsetos et al., 1991; Torbidoni et al., 2015). Using the Y79 and SNUOT-Rb1 cell lines, carboplatin-resistant retinoblastoma cell lines were established in the present study.

The two carboplatin-resistant retinoblastoma cell lines, Y79/CBP and SNUOT-Rb1/CBP, were developed by treating cells with increasing concentrations of carboplatin. The cells were subsequently characterized in terms of the cell cycle kinetics and MDR. The Y79/CBP and SNUOT-Rb1/CBP cells exhibited strong *in vitro* and *in vivo* resistance to carboplatin. They exhibited decreased DNA fragmentation and reduced cleaved caspase-3 expression upon carboplatin treatment when compared with the parental cells. In addition, following intravitreal injection of carboplatin, the tumors formed of the resistant cell lines grew to a larger size compared with the tumors formed of their parental cell lines. Further characterization revealed that this *in vitro* and *in vivo* resistance to carboplatin could be linked to changes in the cell cycle machinery and the MDR-related properties.

The first characteristic of the carboplatin-resistant retinoblastoma cells that was observed in the present study was the

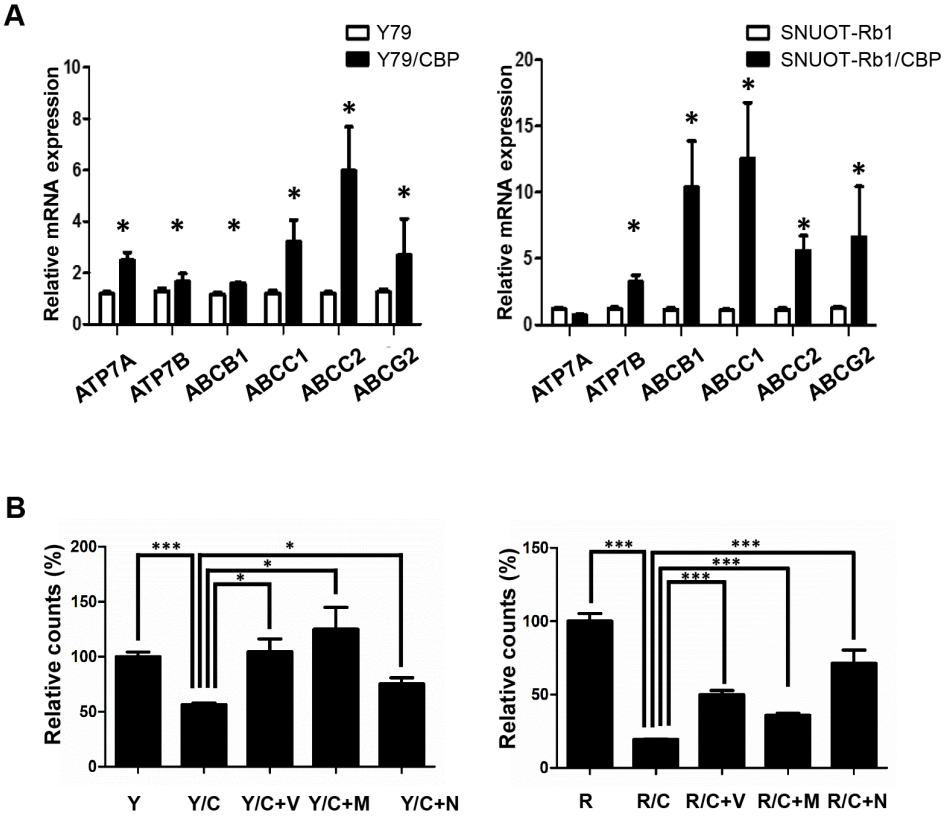

Fig. 4. Increased drug efflux in carboplatin-resistant retinoblastoma cells. (A) Expression of MDR-associated genes. Statistical analysis performed using an unpaired Student's *t*-test. (B) Relative fluorescein intensity of cells in the MDR assay. Statistical analysis was performed using the Student's *t*-test. $*P < 0.05$; $***P < 0.001$. CBP, carboplatin; Y, Y79; Y/C, Y79/CBP; V, verapamil; M, MK571; N, novobiocin; R, SNUOT-Rb1; R/C, SNUOT-Rb1/CBP.

change in their proliferative rate. Y79/CBP and SNUOT-Rb1/CBP cells exhibited decreased growth compared with their parental cells, similar to paclitaxel- or cisplatin-resistant esophageal carcinoma cell lines (Wang et al., 2013; Wen et al., 2009). FACS analysis showed that a greater proportion of the Y79/CBP and SNUOT-Rb1/CBP cells were in the G_0/G_1 phase compared with their parental cells. It is been shown that cisplatin and carboplatin cause DNA damage and induce a potent S-phase arrest (Cruet-Hennequart et al., 2009; Longley and Johnston, 2005). After cell cycle arrest, the cells begin to regenerate by activating or deactivating genes related to DNA repair (Longley and Johnston, 2005). Similarly, the proportion of cells in the G_0/G_1 stage in the Y79/CBP and SNUOT-Rb1/CBP cells was compared with the respective parental cells. In agreement with these results, expression of the cyclin-dependent kinase inhibitors, p18 and p21, was higher in the carboplatin-resistant retinoblastoma cells. This is likely due to the fact that arrest at the G_0/G_1 phase allows for cells to repair any DNA damage and activate the endogenous drug resistance mechanisms. It was also reported that tumor cells in the G_0/G_1 phase exhibited a higher rate of metastasis and higher resistance to anticancer agents than tumor cells in the S/G_2/M phases (Yano et al., 2014).

Another characteristic of the carboplatin-resistant retinoblastoma cells that was reported in the present study was the increased expression of MDR-related genes. An MDR assay was performed using a hydrophobic dye that is pumped out of the cell by the ABC transporters to show that drug efflux was increased in these cells. ABC transporter expression is a key factor in chemotherapeutic resistance (Ishikawa et al., 2010). Members of this superfamily utilize energy from ATP hydrolysis to transport a broad range of substrates, including peptides, lipids and anticancer drugs, across the cell membrane (Wu and Ambudkar, 2014). It has been reported that in several tumor types, forkhead box M1 (FoxM1) promotes drug resistance through the ABC receptor (Hou et al., 2017), and FoxM1 regulates ABCC4 gene transcription to increase carboplatin resistance in Y79CR cells (Zhu et al., 2018). In the present study, Y79/CBP and SNUOT-Rb1/CBP cells exhibited increased expression of genes related to ABC transporters and drug efflux, and it was confirmed that FoxM1 and ABCC4 gene expression also increased (Supplementary Fig. S6).

Another potential cause of chemotherapy resistance is the presence of Cu transporters. It has been reported that two Cu efflux transporters, ATP7A and ATP7B, regulate the uptake of platinum agents (cisplatin, carboplatin and oxaliplatin) into tumor cells (Safaei and Howell, 2005). Overexpression of *ATP7A* in ovarian cancer cell lines increases resistance to cisplatin, carboplatin and oxaliplatin (Samimi et al., 2004). In another report, *ATP7B* overexpression in ovarian cancer cell lines resulted in resistance to carboplatin, copper and cisplatin (Katano et al., 2003). Similarly, increased expression of *ATP7A* and *ATP7B* in the Y79/CBP and SNUOT-Rb1/CBP retinoblastoma cell lines may have contributed to the increased carboplatin resistance observed in the present study. In agreement with previous studies demonstrating the importance of MDR-related factors in the therapeutic response in retinoblastoma (Chan et al., 1991; 1997), upregulation of MDR-related genes in the carboplatin-resistant retinoblastoma cell lines was one of their key characteristics. Representative treatments for retinoblastoma chemotherapy include vincristine and etoposide. The Y79/CBP and SNUOT-Rb1/CBP cells established in the present study also exhibited increased resistance to these drugs as well (Supplementary Fig. S7).

In conclusion, in the present study, two carboplatin-resistant retinoblastoma cell lines, Y79/CBP and SNUOT-Rb1/CBP, were established, and were shown to exhibit resistance to several commonly used chemotherapeutics. These cell lines may serve as useful tools in the development of novel treatment options for the treatment of chemoresistant retinoblastoma.

Note: Supplementary information is available on the Molecules and Cells website (www.molcells.org).

ACKNOWLEDGMENTS

This work was supported by the Development of Platform Technology for Innovative Medical Measurement funded by Korea Research Institute of Standards and Science (KRISS-GP2022-0006), The Bio & Medical Technology Development Program of the National Research Foundation, MSIP (No. 2018M3D1A1058826), and the Seoul National University Hospital Research (No. 04-2019-0280).

AUTHOR CONTRIBUTIONS

C.S.C. performed the experiments and wrote the manuscript. D.H.J. wrote and revised the manuscript. J.H.K. (Jin Hyoung Kim) reviewed the manuscript. J.H.K. (Jeong Hun Kim) designed the study and wrote the manuscript. All authors have read and approved the final manuscript.

CONFLICT OF INTEREST

The authors have no potential conflicts of interest to disclose.

ORCID

Chang Sik Cho https://orcid.org/0000-0002-0812-1515
Dong Hyun Jo https://orcid.org/0000-0002-6320-6829
Jin Hyoung Kim https://orcid.org/0000-0002-7230-8851
Jeong Hun Kim https://orcid.org/0000-0003-2957-1766

REFERENCES

Abramson, D.H., Shields, C.L., Munier, F.L., and Chantada, G.L. (2015). Treatment of retinoblastoma in 2015: agreement and disagreement. JAMA Ophthalmol. *133*, 1341-1347.

Asada, N., Tsuchiya, H., Ueda, Y., and Tomita, K. (1998). Establishment and characterization of an acquired cisplatin-resistant subline in a human osteosarcoma cell line. Anticancer Res. 18(3A), 1765-1768.

Behrens, B.C., Hamilton, T.C., Masuda, H., Grotzinger, K.R., Whang-Peng, J., Louie, K.G., Knutsen, T., McKoy, W.M., Young, R.C., and Ozols, R.F. (1987). Characterization of a cis-diamminedichloroplatinum(II)-resistant human ovarian cancer cell line and its use in evaluation of platinum analogues. Cancer Res. *47*, 414-418.

Bond, W.S., Akinfenwa, P.Y., Perlaky, L., Hurwitz, M.Y., Hurwitz, R.L., and Chevez-Barrios, P. (2013). Tumorspheres but not adherent cells derived from retinoblastoma tumors are of malignant origin. PLoS One *8*, e63519.

Chan, H.S., Lu, Y., Grogan, T.M., Haddad, G., Hipfner, D.R., Cole, S.P., Deeley, R.G., Ling, V., and Gallie, B.L. (1997). Multidrug resistance protein

(MRP) expression in retinoblastoma correlates with the rare failure of chemotherapy despite cyclosporine for reversal of P-glycoprotein. Cancer Res. *57*, 2325-2330.

Chan, H.S., Thorner, P.S., Haddad, G., and Gallie, B.L. (1991). Multidrug-resistant phenotype in retinoblastoma correlates with P-glycoprotein expression. Ophthalmology *98*, 1425-1431.

Chen, S.Y., Hu, S.S., Dong, Q., Cai, J.X., Zhang, W.P., Sun, J.Y., Wang, T.T., Xie, J., He, H.R., Xing, J.F., et al. (2013). Establishment of paclitaxel-resistant breast cancer cell line and nude mice models, and underlying multidrug resistance mechanisms in vitro and in vivo. Asian Pac. J. Cancer Prev. *14*, 6135-6140.

Cruet-Hennequart, S., Villalan, S., Kaczmarczyk, A., O'Meara, E., Sokol, A.M., and Carty, M.P. (2009). Characterization of the effects of cisplatin and carboplatin on cell cycle progression and DNA damage response activation in DNA polymerase eta-deficient human cells. Cell Cycle *8*, 3039-3050.

Dallas, N.A., Xia, L., Fan, F., Gray, M.J., Gaur, P., van Buren, G., 2nd, Samuel, S., Kim, M.P., Lim, S.J., and Ellis, L.M. (2009). Chemoresistant colorectal cancer cells, the cancer stem cell phenotype, and increased sensitivity to insulin-like growth factor-I receptor inhibition. Cancer Res. *69*, 1951-1957.

Glubrecht, D.D., Kim, J.H., Russell, L., Bamforth, J.S., and Godbout, R. (2009). Differential CRX and OTX2 expression in human retina and retinoblastoma. J. Neurochem. *111*, 250-263.

Hou, Y., Zhu, Q., Li, Z., Peng, Y., Yu, X., Yuan, B., Liu, Y., Liu, Y., Yin, L., Peng, Y., et al. (2017). The FOXM1–ABCC5 axis contributes to paclitaxel resistance in nasopharyngeal carcinoma cells. Cell Death Dis. *8*, e2659.

Ishikawa, Y., Nagai, J., Okada, Y., Sato, K., Yumoto, R., and Takano, M. (2010). Function and expression of ATP-binding cassette transporters in cultured human Y79 retinoblastoma cells. Biol. Pharm. Bull. *33*, 504-511.

Jensen, N.F., Stenvang, J., Beck, M.K., Hanáková, B., Belling, K.C., Do, K.N., Viuff, B., Nygård, S.B., Gupta, R., Rasmussen, M.H., et al. (2015). Establishment and characterization of models of chemotherapy resistance in colorectal cancer: towards a predictive signature of chemoresistance. Mol. Oncol. *9*, 1169-1185.

Jo, D.H., Lee, K., Kim, J.H., Jun, H.O., Kim, Y., Cho, Y.L., Yu, Y.S., Min, J.K., and Kim, J.H. (2017). L1 increases adhesion-mediated proliferation and chemoresistance of retinoblastoma. Oncotarget *8*, 15441-15452.

Jo, D.H., Son, D., Na, Y., Jang, M., Choi, J.H., Kim, J.H., Yu, Y.S., Seok, S.H., and Kim, J.H. (2013). Orthotopic transplantation of retinoblastoma cells into vitreous cavity of zebrafish for screening of anticancer drugs. Mol. Cancer *12*, 71.

Kaliki, S. and Shields, C.L. (2015). Retinoblastoma: achieving new standards with methods of chemotherapy. Indian J. Ophthalmol. *63*, 103-109.

Kaplan, H.J., Chiang, C.W., Chen, J., and Song, S.K. (2010). Vitreous volume of the mouse measured by quantitative high-resolution MRI. Invest. Ophthalmol. Vis. Sci. *51*, 4414.

Katano, K., Safaei, R., Samimi, G., Holzer, A., Rochdi, M., and Howell, S.B. (2003). The copper export pump ATP7B modulates the cellular pharmacology of carboplatin in ovarian carcinoma cells. Mol. Pharmacol. *64*, 466-473.

Katsetos, C.D., Herman, M.M., Frankfurter, A., Uffer, S., Perentes, E., and Rubinstein, L.J. (1991). Neuron-associated class III beta-tubulin isotype, microtubule-associated protein 2, and synaptophysin in human retinoblastomas in situ. Further immunohistochemical observations on the Flexner-Wintersteiner rosettes. Lab. Invest. *64*, 45-54.

Khokhlova, O.N., Tukhovskaya, E.A., Kravchenko, I.N., Sadovnikova, E.S., Pakhomova, I.A., Kalabina, E.A., Lobanov, A.V., Shaykhutdinova, E.R., Ismailova, A.M., and Murashev, A.N. (2017). Using tiletamine-zolazepam-xylazine anesthesia compared to CO2-inhalation for terminal clinical chemistry, hematology, and coagulation analysis in mice. J. Pharmacol. Toxicol. Methods *84*, 11-19.

Kim, J.H., Kim, J.H., Yu, Y.S., Kim, D.H., Kim, C.J., and Kim, K.W. (2007). Establishment and characterization of a novel, spontaneously immortalized retinoblastoma cell line with adherent growth. Int. J. Oncol. *31*, 585-592.

Laurie, N., Mohan, A., McEvoy, J., Reed, D., Zhang, J., Schweers, B., Ajioka, I., Valentine, V., Johnson, D., Ellison, D., et al. (2009). Changes in retinoblastoma cell adhesion associated with optic nerve invasion. Mol. Cell. Biol. *29*, 6268-6282.

Laurie, N.A., Gray, J.K., Zhang, J., Leggas, M., Relling, M., Egorin, M., Stewart, C., and Dyer, M.A. (2005). Topotecan combination chemotherapy in two new rodent models of retinoblastoma. Clin. Cancer Res. *11*, 7569-7578.

Longley, D.B. and Johnston, P.G. (2005). Molecular mechanisms of drug resistance. J. Pathol. *205*, 275-292.

Safaei, R. and Howell, S.B. (2005). Copper transporters regulate the cellular pharmacology and sensitivity to Pt drugs. Crit. Rev. Oncol. Hematol. *53*, 13-23.

Samimi, G., Safaei, R., Katano, K., Holzer, A.K., Rochdi, M., Tomioka, M., Goodman, M., and Howell, S.B. (2004). Increased expression of the copper efflux transporter ATP7A mediates resistance to cisplatin, carboplatin, and oxaliplatin in ovarian cancer cells. Clin. Cancer Res. *10*, 4661-4669.

Stephan, H., Boeloeni, R., Eggert, A., Bornfeld, N., and Schueler, A. (2008). Photodynamic therapy in retinoblastoma: effects of verteporfin on retinoblastoma cell lines. Invest. Ophthalmol. Vis. Sci. *49*, 3158-3163.

Torbidoni, A.V., Laurent, V.E., Sampor, C., Ottaviani, D., Vazquez, V., Gabri, M.R., Rossi, J., de Dávila, M.T., Alonso, C., Alonso, D.F., et al. (2015). Association of cone-rod homeobox transcription factor messenger RNA with pediatric metastatic retinoblastoma. JAMA Ophthalmol. *133*, 805-812.

Wang, C., Guo, L.B., Ma, J.Y., Li, Y.M., and Liu, H.M. (2013). Establishment and characterization of a paclitaxelresistant human esophageal carcinoma cell line. Int. J. Oncol. *43*, 1607-1617.

Wang, Y.F., Kunda, P.E., Lin, J.W., Wang, H., Chen, X.M., Liu, Q.L., and Liu, T. (2013). Cytokine-induced killer cells co-cultured with complete tumor antigen-loaded dendritic cells, have enhanced selective cytotoxicity on carboplatin-resistant retinoblastoma cells. Oncol. Rep. *29*, 1841-1850.

Wen, J., Zheng, B., Hu, Y., Zhang, X., Yang, H., Luo, K.J., Zhang, X., Li, Y.F., and Fu, J.H. (2009). Establishment and biological analysis of the EC109/CDDP multidrug-resistant esophageal squamous cell carcinoma cell line. Oncol. Rep. *22*, 65-71.

Wu, C.P. and Ambudkar, S.V. (2014). The pharmacological impact of ATP-binding cassette drug transporters on vemurafenib-based therapy. Acta Pharm. Sin. B *4*, 105-111.

Yano, S., Miwa, S., Mii, S., Hiroshima, Y., Uehara, F., Yamamoto, M., Kishimoto, H., Tazawa, H., Bouvet, M., Fujiwara, T., et al. (2014). Invading cancer cells are predominantly in G0/G1 resulting in chemoresistance demonstrated by real-time FUCCI imaging. Cell Cycle *13*, 953-960.

Zhu, X., Xue, L., Yao, Y., Wang, K., Tan, C., Zhuang, M., Zhou, F., and Zhu, L. (2018). The FoxM1-ABCC4 axis mediates carboplatin resistance in human retinoblastoma Y-79 cells. Acta Biochim. Biophys. Sin. (Shanghai) *50*, 914-920.